

Supplementary material for

Variation in the biomolecular interactions of nickel(II) hydrazone complexes upon tuning the hydrazide fragment

Paramasivam Krishnamoorthy,^a Palanisamy Sathyadevi,^a Rachel R. Butorac,^b Alan H. Cowley,^b Nattamai S.P. Bhuvanesh,^c and Nallasamy Dharmaraj^{a,*}

^a *Department of Chemistry, Bharathiar University, Coimbatore - 641 046, India*

E-mail address: dharmaraj@buc.edu.in; Tel.: +91 422 2428316; Fax: +91 422 2422387

^b *Department of Chemistry and Biochemistry, University of Texas at Austin, Austin, Texas 78712, U.S.A*

^c *Department of Chemistry, Texas A&M University, College Station, TX 77843, U.S.A.*

Figures

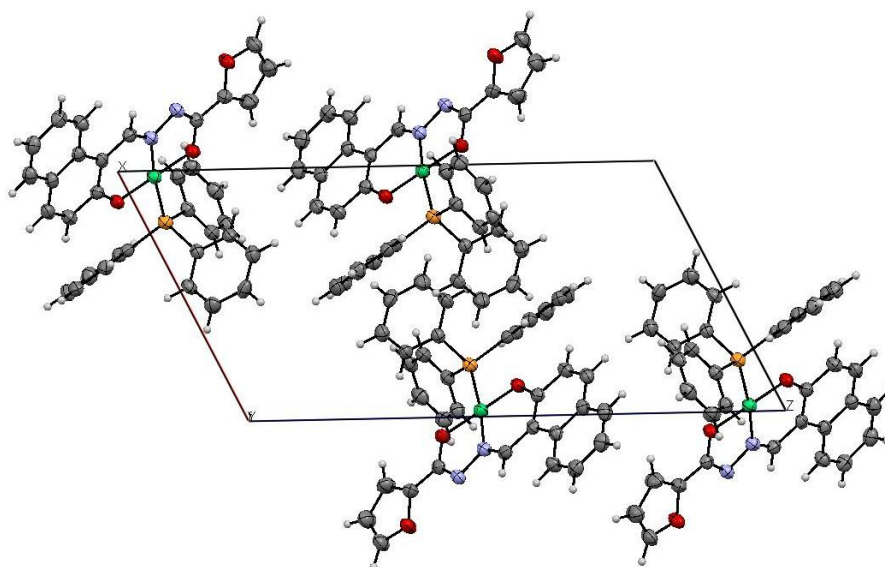


Figure S1. Unit cell packing diagram of the complex 4.

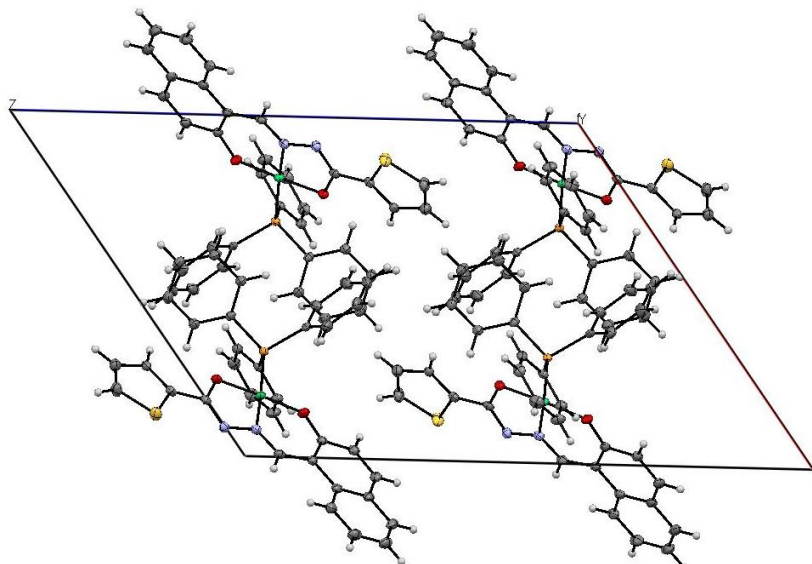


Figure S2. Unit cell packing diagram of the complex 5.

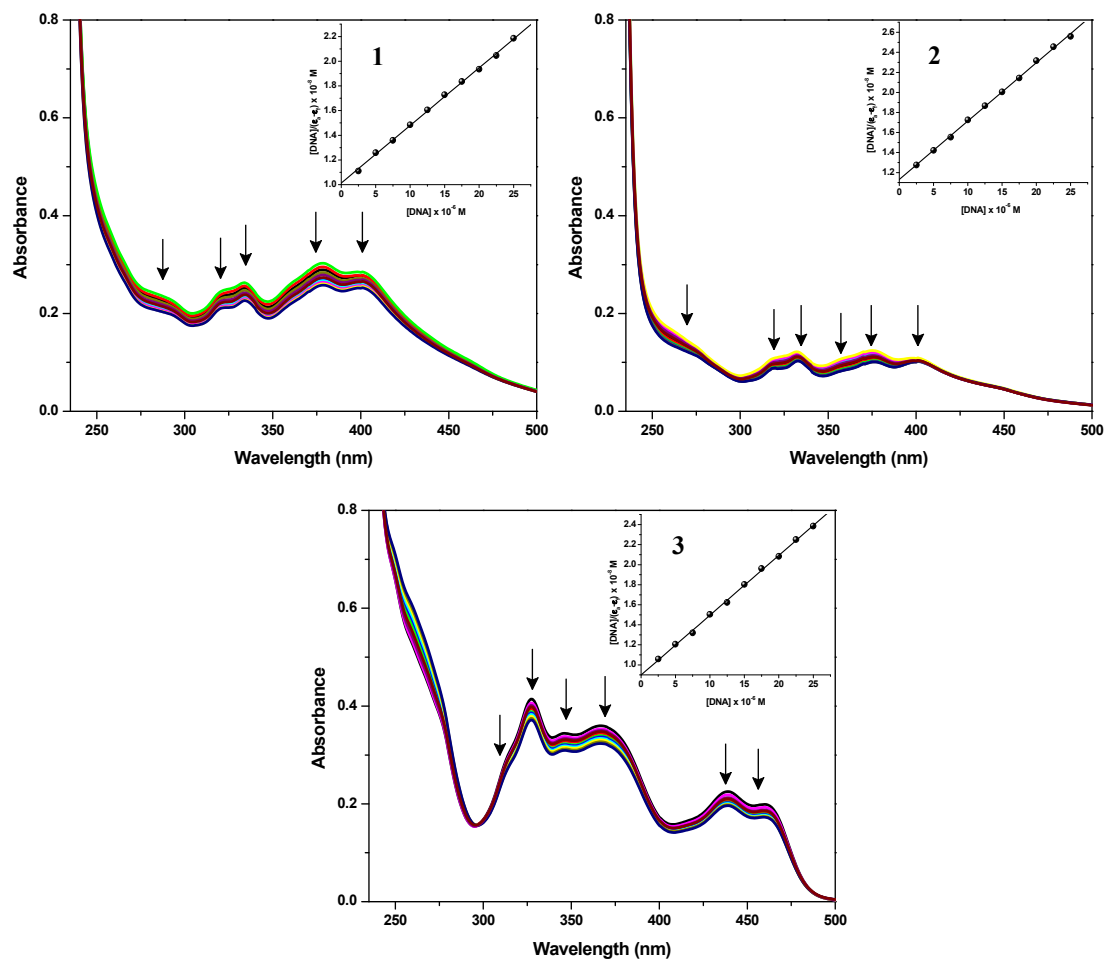


Figure S3. Electronic absorption spectra of ligands **1-3** (25 μM) in the absence and presence of increasing amounts of CT DNA (2.5, 5.0, 7.5, 10.0, 12.5, 15.0, 17.5 and 20.0, 22.5 and 25 μM). Arrows show the changes in absorbance as a function of increasing DNA concentration (Inset: Plot of $[\text{DNA}]$ vs $[\text{DNA}]/(\epsilon_a - \epsilon_f)$).

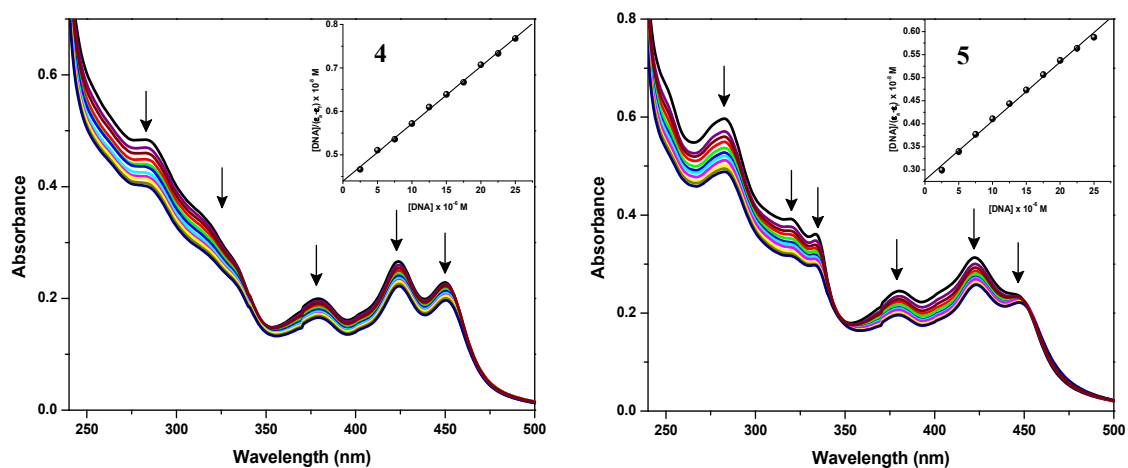


Figure S4. Electronic absorption spectra of complexes **4** and **5** (25 μM) in the absence and presence of increasing amounts of CT DNA (2.5, 5.0, 7.5, 10.0, 12.5, 15.0, 17.5 and 20.0, 22.5 and 25 μM). Arrows show the changes in absorbance as a function of increasing DNA concentration (Inset: Plot of $[\text{DNA}]$ vs $[\text{DNA}]/(\epsilon_a - \epsilon_f)$).

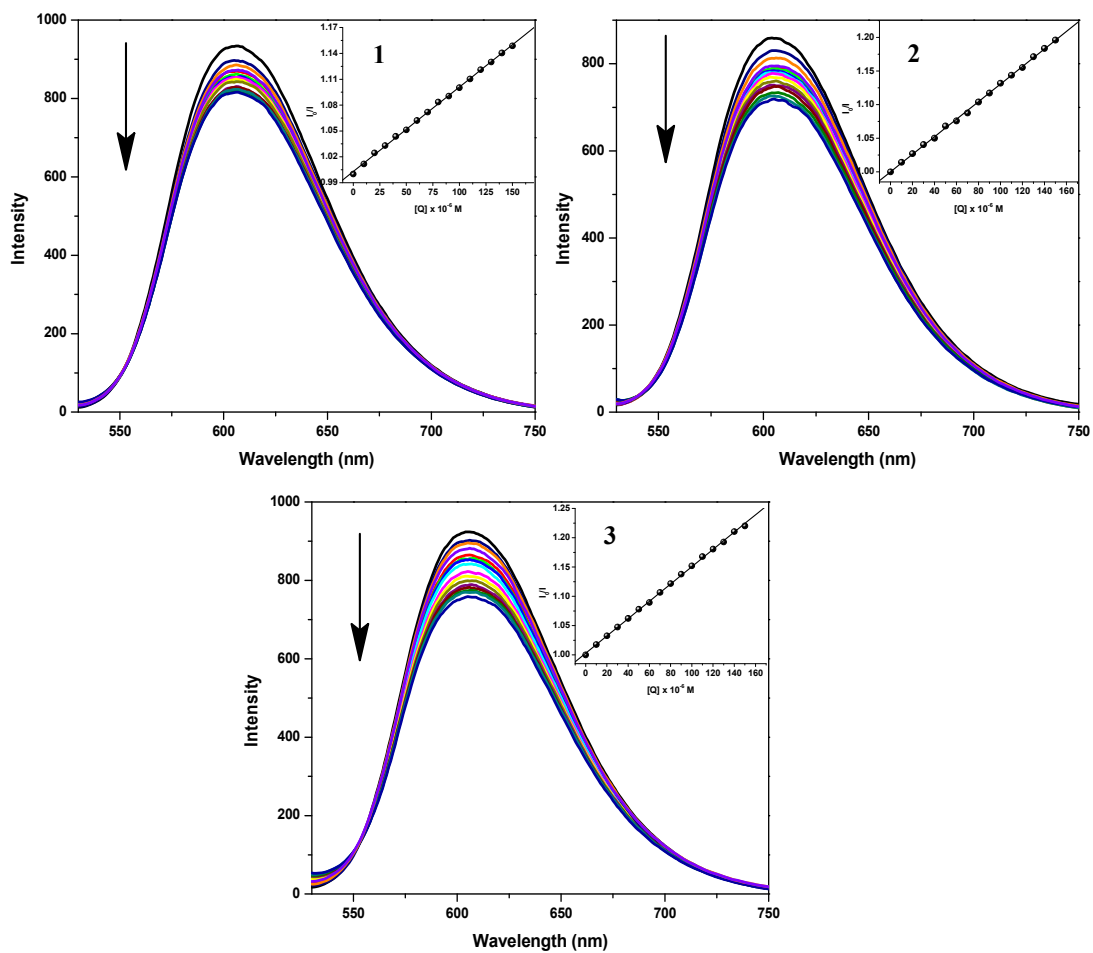


Figure S5. Emission spectra of DNA-EB, in the presence of 0, 10, 20, 30, 40, 50, 60, 70, 80, 90, 100, 110, 120, 130, 140 and 150 μM of ligands **1-3**. Arrow indicates the change in the emission intensity as a function of ligand concentration (Inset: Stern-Volmer plot of the fluorescence titration data corresponding to the ligands).

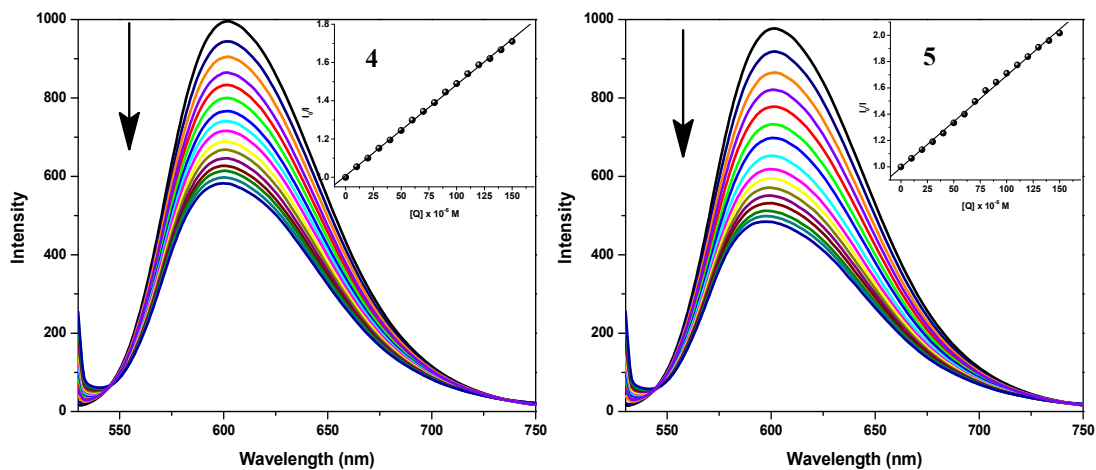


Figure S6. Emission spectra of DNA-EB, in the presence of 0, 10, 20, 30, 40, 50, 60, 70, 80, 90, 100, 110, 120, 130, 140 and 150 μM of complexes **4** and **5**. Arrow indicates the change in the emission intensity as a function of complex concentration (Inset: Stern-Volmer plot of the fluorescence titration data corresponding to the complex).

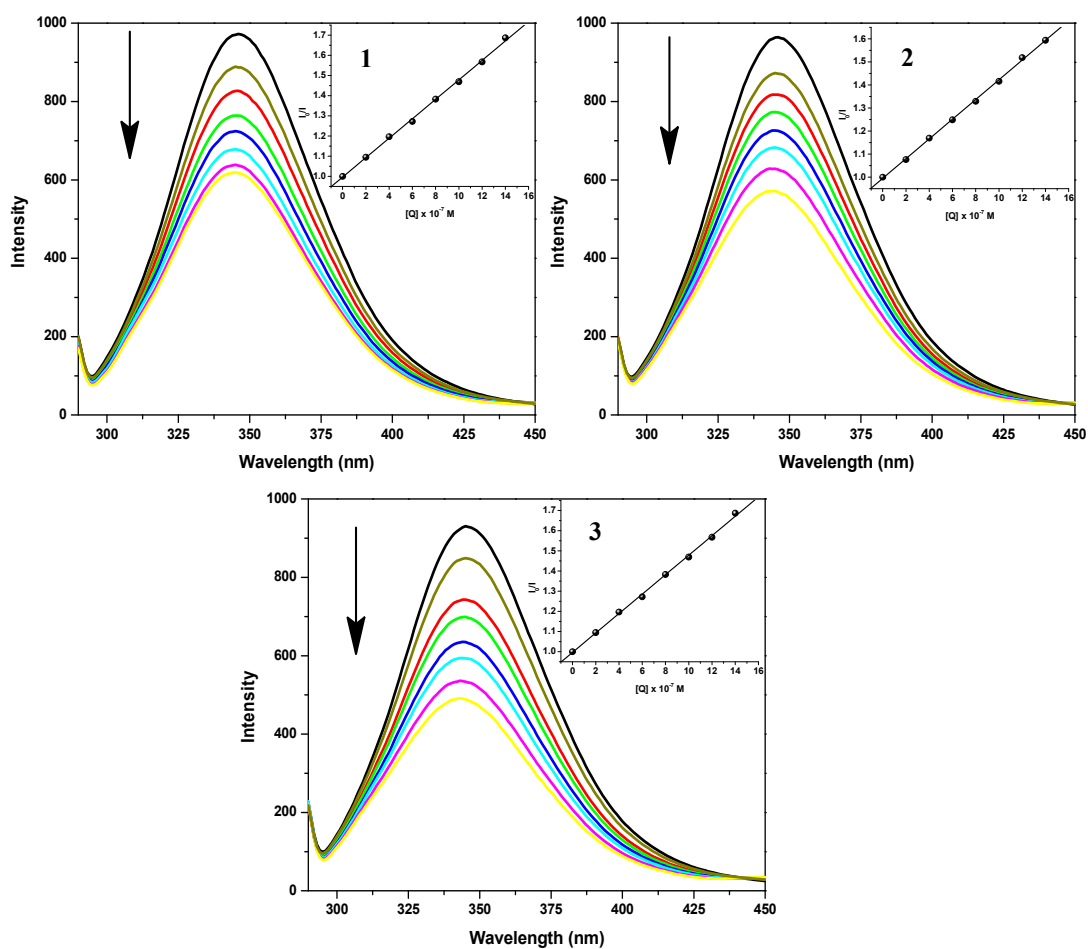


Figure S7. Emission spectra of BSA (1×10^{-6} M; $\lambda_{\text{exi}} = 280$ nm; $\lambda_{\text{emi}} = 345$ nm) as a function of concentration of the ligands **1-3** ($0, 2, 4, 6, 8, 10, 12$ and 14×10^{-7} M). Arrow indicates the effect of the ligands on the fluorescence emission of BSA (Inset: Plot between $[Q]$ and I_0/I).

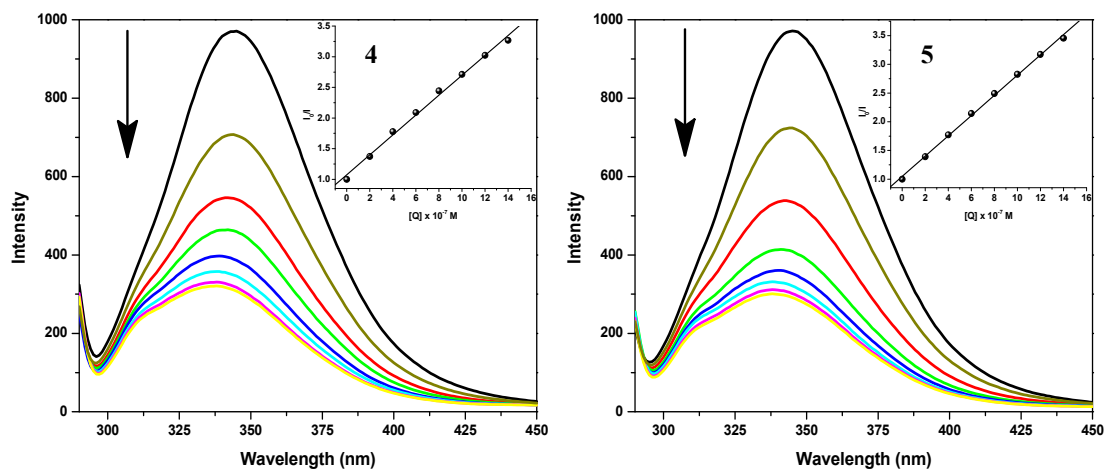


Figure S8. Emission spectra of BSA (1×10^{-6} M; $\lambda_{\text{exi}} = 280$ nm; $\lambda_{\text{emi}} = 345$ nm) as a function of concentration of the complexes **4** and **5** ($0, 2, 4, 6, 8, 10, 12$ and 14×10^{-7} M). Arrow indicates the effect of metal complexes **4** and **5** on the fluorescence emission of BSA (Inset: Plot between $[Q]$ and I_0/I).

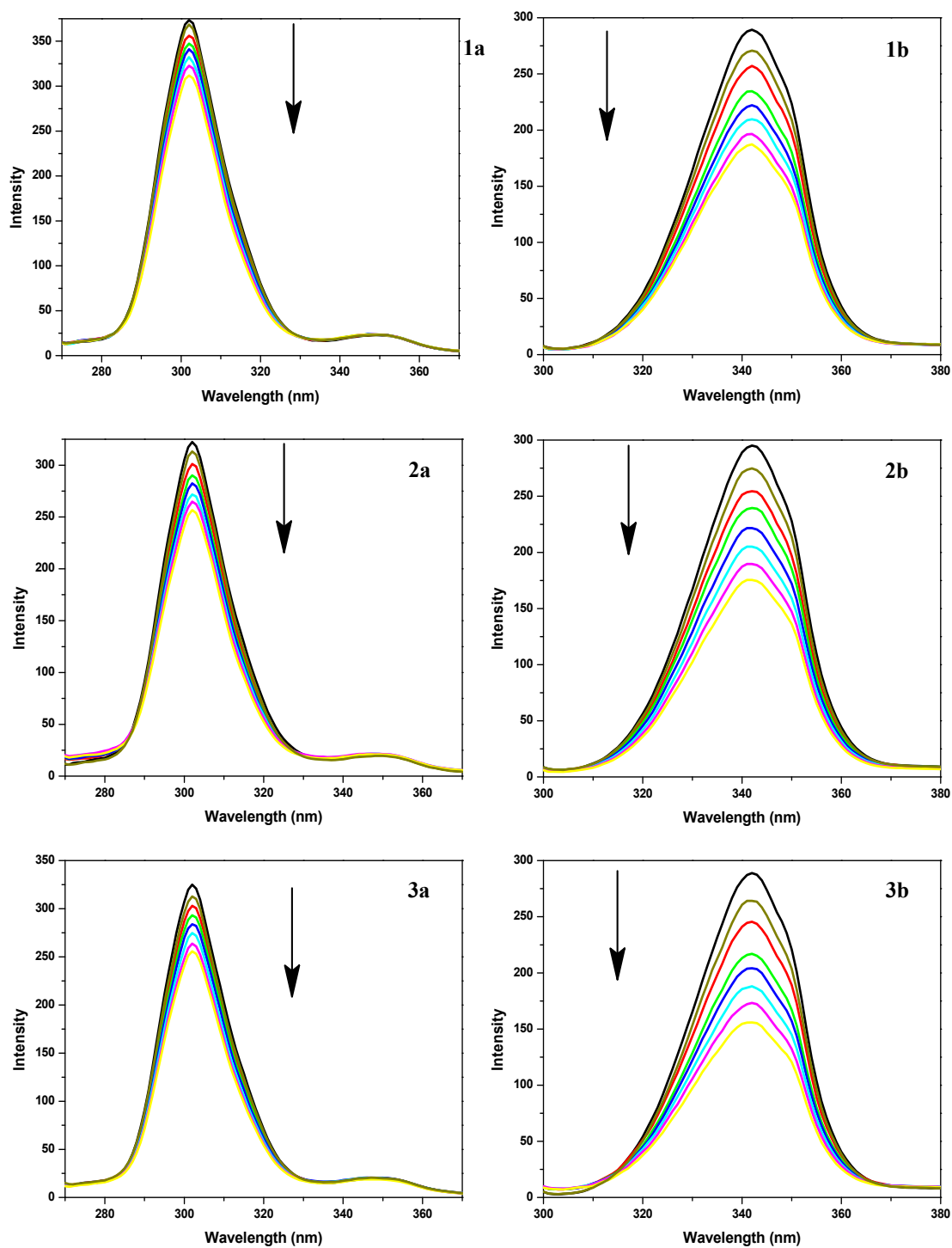


Figure S9. Synchronous spectra of BSA (1×10^{-6} M) as a function of concentration of the ligands **1-3** ($0, 2, 4, 6, 8, 10, 12$ and 14×10^{-7} M) with wavelength difference of $\Delta\lambda = 15$ nm (a) and $\Delta\lambda = 60$ nm (b). Arrow indicates the change in emission intensity w.r.t various concentration of the ligands.

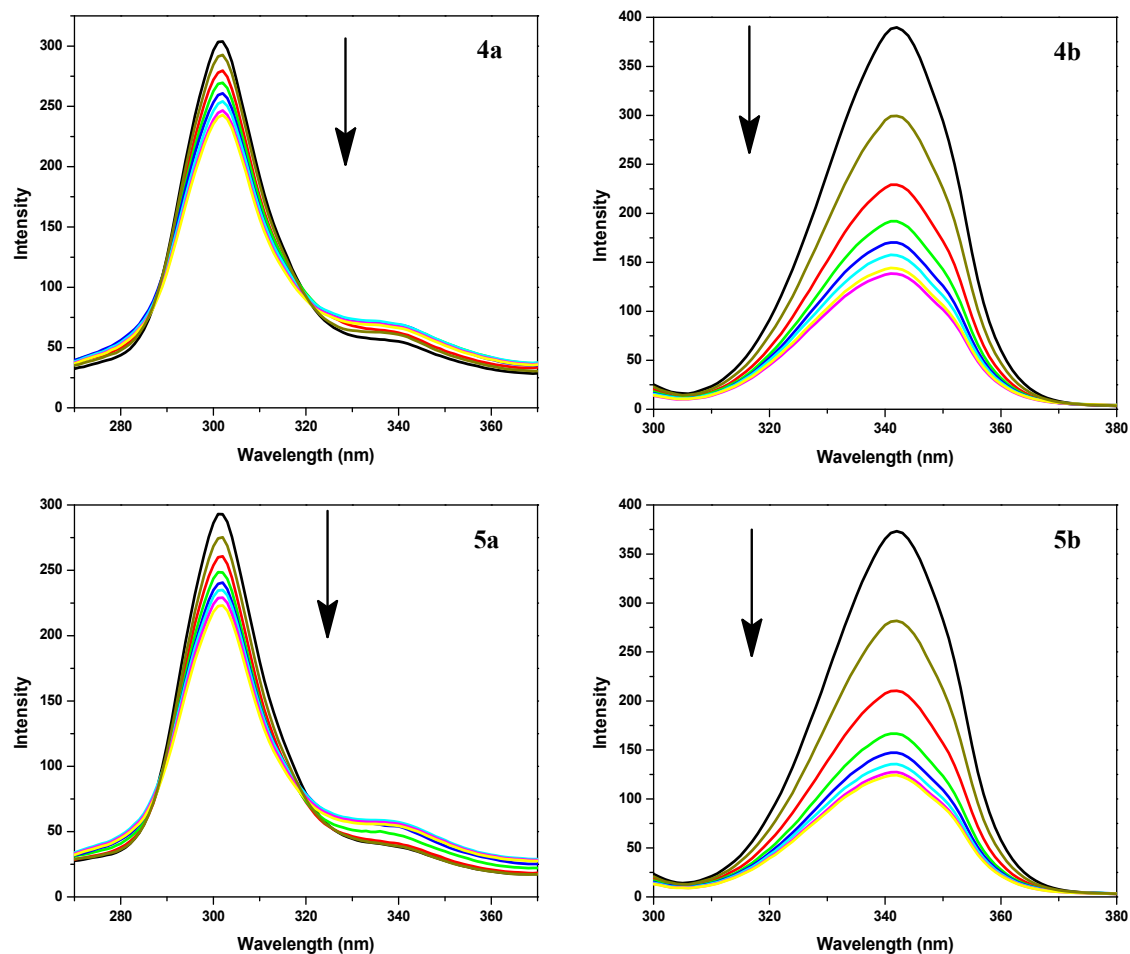


Figure S10. Synchronous spectra of BSA (1×10^{-6} M) as a function of concentration of the complexes **4** and **5** ($0, 2, 4, 6, 8, 10, 12$ and 14×10^{-7} M) with wavelength difference of $\Delta\lambda = 15$ nm (a) and $\Delta\lambda = 60$ nm (b). Arrow indicates the change in emission intensity w.r.t various concentration of the complexes.

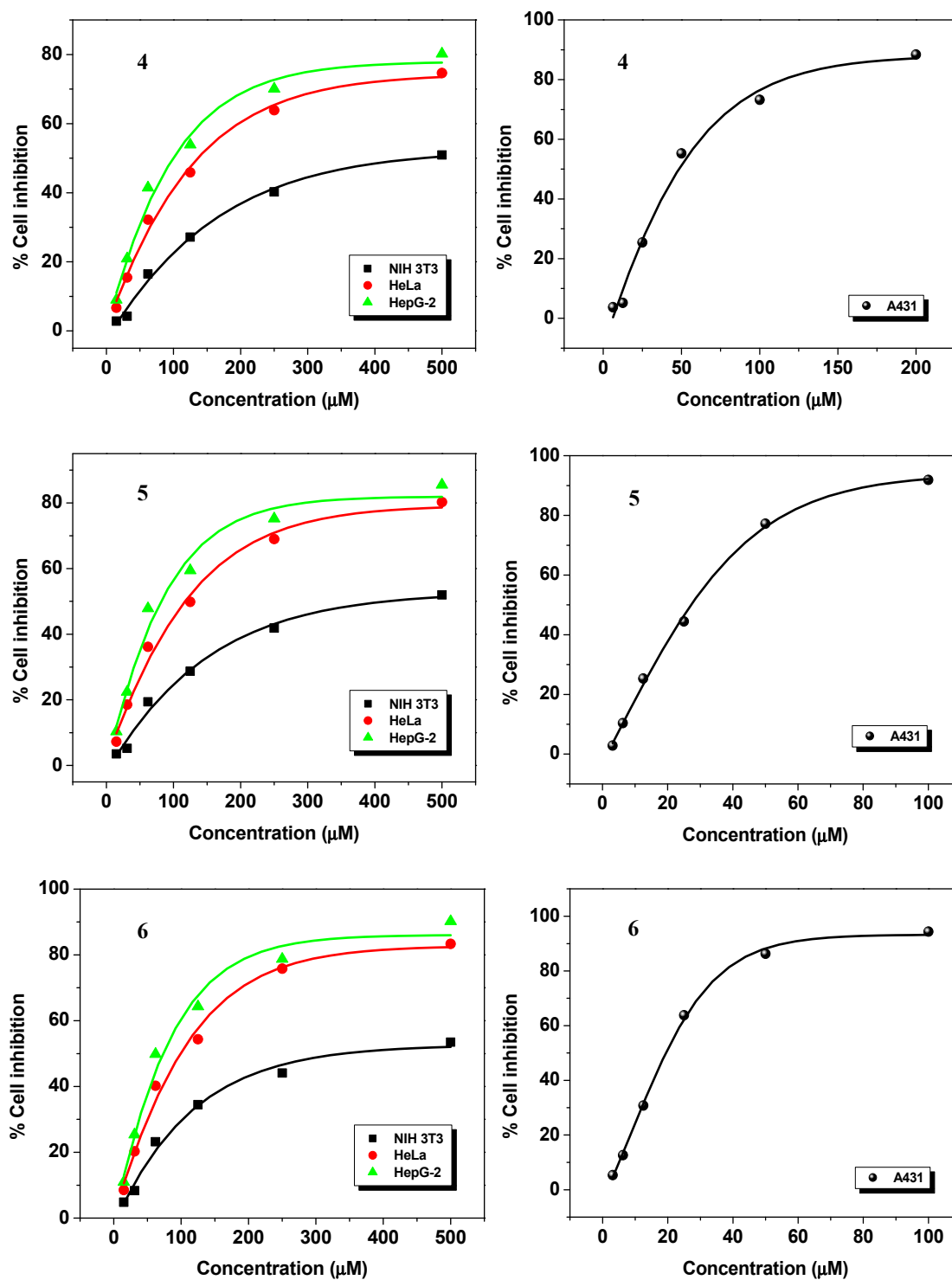


Figure S11. % Cell inhibition of NIH 3T3, HeLa, HepG-2 and A431 cell lines as a function of concentration of nickel hydrazones 4, 5 and 6.